Journal of Hydrology 385 (2010) 279–291

Contents lists available at ScienceDirect

Journal of Hydrology

journal homepage: www.elsevier.com/locate/jhydrol

Statistical downscaling of river flows

Clement Tisseuil [a,*], Mathieu Vrac [b], Sovan Lek [a], Andrew J. Wade [c]

[a] Université de Toulouse, UMR CNRS-UPS 5174, Evolution et Diversité Biologique (EDB), 118 route de Narbonne, 31062 Toulouse Cedex 4, France
[b] Laboratoire des Sciences du Climat et de l'Environnement (LSCE-IPSL) CNRS/CEA/UVSQ, Centre d'étude de Saclay, Orme des Merisiers, Bat. 701 91191 Gif-sur-Yvette, France
[c] Aquatic Environments Research Centre, School of Human and Environmental Sciences, University of Reading, RG6 6AB, UK

ARTICLE INFO

Article history:
Received 1 June 2009
Received in revised form 18 November 2009
Accepted 23 February 2010

This manuscript was handled by
Dr. A. Bardossy, Editor-in-Chief, with the
assistance of K.P. Sudheer, Associate Editor

Keywords:
Hydrological regimes
Generalized linear models
Generalized additive models
Boosted trees
Neural networks
Global climate models

SUMMARY

An extensive statistical 'downscaling' study is done to relate large-scale climate information from a general circulation model (GCM) to local-scale river flows in SW France for 51 gauging stations ranging from nival (snow-dominated) to pluvial (rainfall-dominated) river-systems. This study helps to select the appropriate statistical method at a given spatial and temporal scale to downscale hydrology for future climate change impact assessment of hydrological resources. The four proposed statistical downscaling models use large-scale predictors (derived from climate model outputs or reanalysis data) that characterize precipitation and evaporation processes in the hydrological cycle to estimate summary flow statistics. The four statistical models used are generalized linear (GLM) and additive (GAM) models, aggregated boosted trees (ABT) and multi-layer perceptron neural networks (ANN). These four models were each applied at two different spatial scales, namely at that of a single flow-gauging station (local downscaling) and that of a group of flow-gauging stations having the same hydrological behaviour (regional downscaling). For each statistical model and each spatial resolution, three temporal resolutions were considered, namely the daily mean flows, the summary statistics of fortnightly flows and a daily 'integrated approach'. The results show that flow sensitivity to atmospheric factors is significantly different between nival and pluvial hydrological systems which are mainly influenced, respectively, by shortwave solar radiations and atmospheric temperature. The non-linear models (i.e. GAM, ABT and ANN) performed better than the linear GLM when simulating fortnightly flow percentiles. The aggregated boosted trees method showed higher and less variable R^2 values to downscale the hydrological variability in both nival and pluvial regimes. Based on GCM cnrm-cm3 and scenarios A2 and A1B, future relative changes of fortnightly median flows were projected based on the regional downscaling approach. The results suggest a global decrease of flow in both pluvial and nival regimes, especially in spring, summer and autumn, whatever the considered scenario. The discussion considers the performance of each statistical method for downscaling flow at different spatial and temporal scales as well as the relationship between atmospheric processes and flow variability.

Introduction

Climate change is expected to adversely impact water resources, water quality and the freshwater ecology and therefore methods are required to quantify the likely impacts to develop mitigation and adaptation strategies (Whitehead et al., 2009). Such quantification requires an ability to forecast river flow based on the projected changes in climate to assess changes in flow-pathways, pollutant source area, dilution and residence times, all of which affect the water quality and the aquatic ecosystem. Classically, future climate change is modeled under several hypothetical scenarios using general circulation models (GCM) which are mechanistic models built to physically represent the main atmospheric processes. However, GCM remain relatively coarse in resolution (approximately 2.5° × 2.5°, i.e. about 250 km × 250 km) and are unable to resolve sub-grid scale features such as topography, clouds and land use. This represents a considerable problem for the impact assessment of climate change on hydrological dynamics in river-systems. Thus, considerable efforts in the climate community have focused on the development of techniques, the so called 'downscaling' step, to bridge the gap between large- and local-scale climate data. To date, impact studies of climate change on hydrology involve a two-step approach: (i) GCM outputs are used to generate local climate conditions such as precipitation and temperature, which is known as 'downscaling', then; (ii) these downscaled local climate data are used as input to a hydrological model to project the hydrological changes according to future climate. Fowler et al. (2007) made a comparative review of downscaling models applied to hydrological studies, which are usually

* Corresponding author. Tel.: +33 5 61 55 67 35; fax: +33 5 61 55 67 28.
E-mail address: clement.tisseuil@gmail.com (C. Tisseuil).

0022-1694/$ - see front matter © 2010 Elsevier B.V. All rights reserved.
doi:10.1016/j.jhydrol.2010.02.030

separated into either dynamical or statistical approaches. Dynamical downscaling is performed through regional climate models (RCMs) which physically simulate the smaller-scale dynamical processes that control climate at the regional level down to 5 km × 5 km. GCM outputs are used to define the boundary conditions of RCMs. However, RCMs are computationally expensive in the production of the regional simulations. As such, it is currently possible to apply RCMs to limited periods and regions only.

This study relies on statistical downscaling models (SDMs). Based on observed data, SDMs define relationships between the large-scale variable fields, derived either from climate model outputs or observations, and local-scale surface conditions. The large-scale variable fields from GCMs or reanalysis data (the predictors) are chosen such that they are strongly related to the local-scale conditions of interest (the predictands or response variable). The relationships can then be used to estimate changes in river flow, or other local hydrological measures such as precipitation or air temperature, based on future projections from global or regional climate models. SDMs are generally separated into three types of approach which can be combined: regression models, weather typing schemes and weather generators (Vrac and Naveau, 2007a). Multiple linear models, in the regression-based approach are the most applied in downscaling, for example the well known SDSM tool (Wilby et al., 2002). These assume a linear relationship between large-scale atmospheric predictors and the response variable. However, several studies have shown that taking into account non-linearity between predictors and the predictand in statistical downscaling can improve the goodness-of-fit (Huth et al., 2008) including polynomial regression (Hewitson, 1994), recursive partitioning tree (Schnur and Lettenmaier, 1998), nearest neighbour (Zorita and von Storch, 1999), artificial neural networks (Harpham and Wilby, 2005; Khan et al., 2006) or generalized additive models (Vrac et al., 2007a; Salameh et al., 2009).

The two-step modelling framework, linking GCM outputs to a hydrological model, is usually constrained in space by the domain of calibration of the hydrological model. Furthermore the data requirement for setting the hydrological model parameters may be large, both for conceptual and fully distributed hydrological models (Arheimer and Wittgren, 1994; Eckhardt et al., 2005; Thompson et al., 2004; Habets et al., 2008). One possibility to increase the spatial extent of forecasting river flow at large spatial scales in response to climate change is to develop SDMs able to simulate instream flows directly from GCM atmospheric variables. Seeking a direct association between river flows and GCM outputs may be relevant to facilitate the generalization and extrapolation of river flow simulations over large spatial scales. In the past, such a direct link has been criticized by some authors because of an over-simplification of the hydrological cycle through a lack of consideration of water stores and transfers within the soils and groundwater of a catchment (Xu, 1999), previous poor performances of SDMs linking directly GCM to flow (Wilby et al., 1999) or simply GCM outputs are deemed inappropriate as direct predictors of river flows (Prudhomme et al., 2002). Furthermore, the direct downscaling to streamflow from GCM atmospheric variables generally do not take into account other important factors affecting the streamflow variability such as the land use and soil cover, assuming deterministically that those factors do change with time.

However during the last decade, the relationship between GCM large-scale atmospheric variables and instream flows has been better described. Kingston et al. (2006) made a useful synthesis of recent integrated hydrological–climate research regarding the links between large-scale atmospheric circulation patterns (e.g., characterizing the North Atlantic Oscillation – NAO), regional climate and streamflow variations in the northern North Atlantic region over the last century and especially the last 50 years. Surprisingly, few studies have investigated such a link between atmospheric circulation patterns and flow in a purely predictive way, e.g., through downscaling applications. Examples include Cannon and Whitfield (2002) who applied an ensemble neural network downscaling approach to 21 watersheds in British Columbia; Ghosh and Mujumdar (2008) who simulated the streamflow of an Indian river for the monsoon period using a relevance vector machine; Landman et al. (2001) who downscaled the seasonal streamflow at the inlets of twelve dams in South Africa from predicted monthly-mean sea-surface temperature fields; Phillips et al. (2003) who used atmospheric circulation patterns and regional climate predictors to generate mean monthly flows in two British rivers; Déry and Wood (2004) who have shown that the recent variability in Hudson Bay river was significantly explained by the Arctic Oscillation over the last decades; Lawler et al. (2003) who investigated the influence of changes in atmospheric circulation and regional climate variability on river flows and suspended sediment fluxes in southern Iceland; and Ye et al. (2004) who used combinations of climate and atmospheric variables to explain from about 31–55% of the variance of the annual total discharges of three Siberian rivers.

In this study, various direct downscaling strategies linking flows to GCM outputs are investigated to estimate the flows measured at 51 hydrological gauging stations located in southwest France, representative of a transition from nival (snow-dominated) to pluvial (rainfall-dominated) hydrological conditions. Reanalysis data from the National Centers for Environmental Prediction and the National Center for Atmospheric Research. (NCEP/NCAR; Kalnay et al., 1996) are used as large-scale atmospheric predictors to calibrate the models and validate the approaches. The focus of this study will address the three following questions:

(1) Which spatial or temporal scale resolution and statistical methods could be the most relevant to downscale the streamflow variability from GCM outputs? As such, the statistical downscaling framework is built upon an extensive comparative approach which has three aspects (Fig. 1, Table 1). Four linear or non-linear statistical methods are applied at two different spatial scales, either to individual stations or regionally to a group of stations, according to three temporal resolutions varying from daily to fortnightly time resolutions.
(2) Can the relationship between climate processes and the hydrological variability be modeled by the downscaling framework according to different hydrological systems? As such, a wide set of NCEP/NCAR atmospheric variables are tested as potential predictors for flows and an extensive sensitivity analysis is performed to quantify the relationship between flows and atmospheric predictors according a range of hydrological regimes from nival to pluvial.
(3) As a synthesis of this work, is the proposed downscaling framework relevant for future climate change impacts studies? As an illustration, future seasonal changes in flows are projected and discussed according to nival and pluvial regimes over the region, using one GCM (cnrm-cm3) and two scenarios (A2, A1B).

Study area and data resource

Mean daily streamflow data for 51 stations located in the southwest of France were obtained from the Hydro2 database maintained by the Ministère de l'Ecologie et du Développement Durable (http://www.hydro.eaufrance.fr/; Table 2; Fig. 2). Three criteria were employed to determine the stations to be selected: (1) a continuous record spanning at least 15 years and starting after 1945; (2) inclusion of a large range of hydrological conditions over the region; (3) gauging stations close to water chemistry and

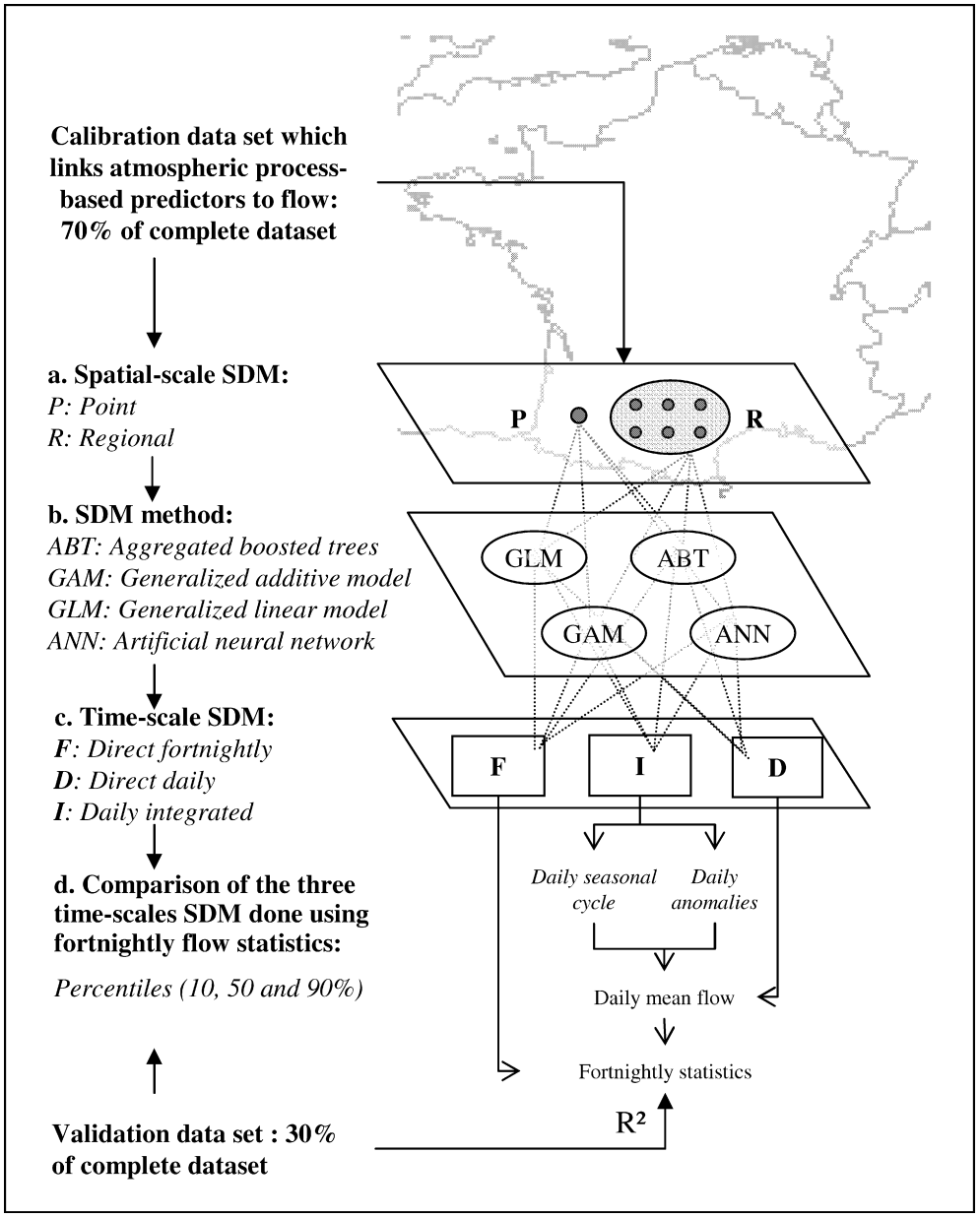

Fig. 1. Statistical downscaling framework. Four different statistical downscaling methods were calibrated using 70% of complete dataset which linked synthesized atmospheric predictors, derived from NCEP/NCAR reanalysis data, to observed flows summarized at different three time scales and point and regional spatial scales. Testing was done using the remaining 30% of the dataset.

Table 1
Abbreviations.

Full name	Abbreviation
Statistical downscaling model	SDM
Generalized linear model	GLM
Generalized additive model	GAM
Aggregated boosted tree	ABT
Artificial neural network	ANN
General circulation model	GCM
Classification and regression trees	CART
Hierarchical ascending clustering	HAC
Principal component analysis	PCA

biological sampling points and therefore of use to investigate the interactions between hydrology, water chemistry and/or biological communities in future studies. In general, the daily flow data from the 51 stations were available from 1968 to 1999.

NCEP/NCAR reanalysis data were used to model the river flows at the 51 gauging stations. NCEP/NCAR reanalysis data are atmospheric model outputs derived from the assimilation of surface observation stations, upper-air stations and satellite-observing platforms with long records starting in 1948 and continuing to present day. These data are typically viewed as 'observed' large-scale data on a regular grid with a spatial resolution of approximately $2.5° \times 2.5°$ (250 km × 250 km). To improve the understanding between atmospheric conditions and flows, 27 atmospheric variables were tested here as potential explanatory variables. These variables included long wave and short wave radiation fluxes, cloud cover, land skin temperature, latent and sensible heat fluxes at surface. The full list is given in Table 3. As this study was built upon a climate change perspective, NCEP/NCAR variables were carefully selected as readily-available GCM outputs (available online at https://esg.llnl.gov:8443/index.jsp) so that these outputs could be used in further studies to generate the flow response to

Table 2
Description of the 51 hydrological gauging stations located SW France with their hydrological regime scales from nival (1) to pluvial (5).

Station ID	Station name	Catchment area (km v)	Longitude (degrees E)	Latitude (degrees N)	Years	Hydrological regimes
O0174010	La Neste d'Aure à Sarrancolin	606	0.38	42.955	1961–1999	1
O0200020	La Garonne	2230	0.707	43.098	1984–1999	1
O0234020	Le Ger à Aspet	95	0.795	43.021	1983–1999	2
O0384010	L'Arac à Soulan	169	1.232	42.899	1962–1999	2
O0444010	Le Lez aux Bordes-sur-Lez	212	1.029	42.903	1971–1999	1
O0502520	Le Salat à Saint-Lizier	1154	1.141	42.991	1974–1999	2
O0624010	Le Volp à Montberaud	91	1.142	43.145	1968–1999	3
O0744030	L'Arize au Mas-d'Azil	218	1.361	43.083	1974–1999	3
O0964030	La Louge au Fousseret	272	1.06	43.267	1970–1999	3
O1712510	L'Ariège à Auterive	3450	1.467	43.369	1966–1999	2
O2034010	L'Aussonnelle à Seilh	192	1.356	43.692	1968–1999	3
O2620010	La Garonne à Verdun-sur-Garonne	13730	1.242	43.855	1972–1999	2
O2883310	La Gimone à Garganvillar	827	1.111	43.998	1965–1999	4
O4142510	L'Agout à Anglès	364	2.596	43.595	1972–1999	4
O4544020	Le Sor à Cambounet-sur-le-Sor	372	2.115	43.577	1977–1999	4
O4704030	Le Dadou à Paulinet	72	2.441	43.822	1968–1999	4
O4984320	Le Tescou à Saint-Nauphary	287	1.432	43.966	1974–1999	3
O5534010	Le Lézert à Saint-Julien-du-Puy	222	2.196	44.162	1968–1999	4
O5685010	La Bonnette à Saint-Antonin-Noble-Val	179	1.748	44.172	1968–1999	4
O5754020	La Vère à Bruniquel	311	1.673	44.024	1971–1999	4
O5964020	Le Lemboulas à Lafrançaise	403	1.203	44.137	1968–1999	4
O6125010	La Petite Barguelonne à Montcuq	62	1.191	44.334	1971–1999	4
O6134010	La Barguelonne à Valence	477	0.998	44.17	1968–1999	5
O6164310	L'Auroue à Caudecoste	196	0.756	44.107	1968–1999	4
O6212530	Le Gers à Panassac	159	0.568	43.383	1965–1999	3
O6312520	Le Gers à Montestruc-sur-Gers	678	0.64	43.791	1965–1999	3
O6692910	La Ba à Nérac	1327	0.335	44.148	1965–1999	4
O6804630	L'Osse à Castex	10.2	0.324	43.399	1965–1999	3
O7971510	Le Lot à Faycelles	6840	2.016	44.557	1979–1999	5
O8133520	Le Célé à Orniac	1194	1.679	44.52	1971–1999	4
O8231510	Le Lot à Cahors	9170	1.446	44.449	1960–1999	5
O8584010	La Lède à Casseneuil	411	0.634	44.446	1970–1999	4
O9000010	La Garonne à Tonneins	51500	0.222	44.412	1989–1999	5
O9034010	Le Tolzac à Varès	255	0.353	44.433	1970–1999	4
O9134010	L'Avance à Montpouillan	405	0.137	44.464	1968–1999	5
P2054010	La Bave à Frayssinhes	183	1.948	44.858	1961–1999	5
P6342510	L'Auvézère à Cherveix-Cubas	586	1.127	45.298	1966–1999	5
P7261510	L'Isle à Abzac	3752	−0.126	45.022	1972–1999	5
P8462510	La Dronne à Coutras	2816	−0.132	45.042	1967–1999	5
Q0100010	L'Adour	272	0.164	43.037	1940–1999	1
Q0280030	L'Adour à Estirac	906	0.029	43.498	1968–1999	2
Q0522520	L'Arros à Gourgue	173	0.259	43.132	1968–1999	3
Q2062510	Le Midour à Laujuzan	256	−0.117	43.821	1966–1999	4
Q2192510	Le Midou à Mont-de-Marsan	800	−0.502	43.892	1967–1998	3
Q4124010	Le Gave d'Héas à Gèdre	84	0.022	42.787	1948–1995	1
Q4801010	Le Gave de Pau à Saint-Pé-de-Bigorre	1120	−0.143	43.103	1955–1999	1
Q5501010	Le Gave de Pau à Bérenx	2575	−0.853	43.509	1940–1999	2
Q6332510	Le Gave d'Aspe à Bedous	425	−0.604	42.981	1948–1999	2
Q7002910	Le Gave d'Oloron à Oloron-Sainte-Marie	1085	−0.608	43.199	1940–1999	2
Q8032510	La Bidouze à A-Camou-Suhast	246	−1.028	43.334	1969–1999	4
S2242510	L'Eyre à Salles	1650	−0.872	44.548	1967–1999	5

projected climate change. Each NCEP/NCAR variable was interpolated to each of the 51 hydrological stations locations using bilinear interpolation. For a given station, the interpolated data result from the weighted average of the data of the nearest points located on the regular grid. Then each interpolated NCEP/NCAR variable was normalized so that its mean was zero and its variance was 1.

Method

The statistical downscaling framework may be summarized in four steps (Fig. 1, Table 1). At step 1, information from the 27 NCEP/NCAR variables was first synthesised into five process-based predictors to be more readily interpreted, namely precipitation, temperature, pressure, radiation and heat flux (see Section "Deriving process-based NCEP/NCAR predictors"; Fig. 3). At step 2, these process-based predictors were used in the statistical downscaling framework (SDM; see Section "Statistical downscaling framework", Fig. 1) to simulate river flow according to two spatial resolutions, namely at a single flow-gauging station or a group of flow-gauging stations having the same hydrological behaviour (Fig. 1a). For each spatial resolution, four statistical models (Fig. 1b) including generalized linear models (GLM), generalized additive models (GAM), aggregated boosted trees (ABT) and artificial neural networks (ANN) were each applied to three temporal resolutions, namely daily mean flow, fortnightly-derived flows statistics (percentiles 10%, 50% and 90%) and a daily integrated approach (Fig. 1c). This daily integrated approach separates the daily flow downscaling process into the downscaling of the daily seasonal cycle, which is defined as the mean flow for each day of the year over the calibration period, and the downscaling of the corresponding daily anomalies which are the values resulting from the subtraction of the daily seasonal cycle from the daily flow data. Performances of the different SDMs are compared between observed and downscaled flow statistics calculated at the fortnightly time scale for each station (Fig. 1d). At step 3, a sensitivity analysis

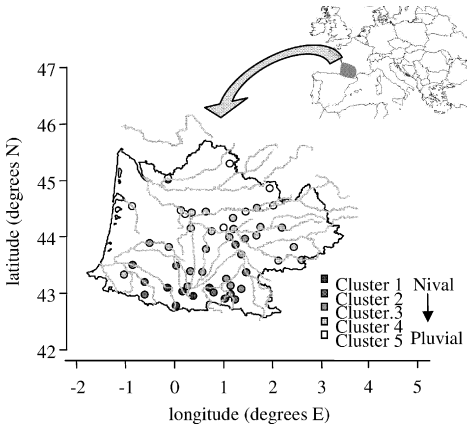

Fig. 2. The locations of the 51 hydrological gauging stations in the Adour-Garonne river-system (SW France). The grey-scale colours represent the hydrological transition from nival (cluster 1) to pluvial (cluster 5) hydrological regimes. Hydrological clusters were identified using HAC.

was performed based on the regional downscaling approach to quantify and describe the relationship between river flow and the five process-based atmospheric variables, according to the hydrological regions and the five statistical methods used (see Section "Sensitivity of downscaled flows to atmospheric predictors"). At step 4, future relative changes of seasonal flow were projected to assess the potential impact of climate change on nival and pluvial systems according to different time periods and future scenarios (see Section "Future projections").

Deriving process-based NCEP/NCAR predictors

The approach was based on a regional, process-based representation of atmospheric variables, which aimed at synthesizing the initial 27 NCEP/NCAR atmospheric variables into a limited number of moderately correlated, physically meaningful, predictors for the downscaling of flows (Fig. 3). With such a representation, correlations between predictors were reduced, so that their relationship with the flow variability could be quantified with more robustness than if using the 27 highly correlated NCEP/NCAR predictors directly. In practice, co-linearity would not impact the performances of the downscaling process; however, the individual contribution of predictors to the flow variance explained, as well as the coefficients estimates in downscaling models, could change erratically. Furthermore, limiting the number of atmospheric predictors reduces the computation time for downscaling models. The method to derive the process-based factors is based on two-steps:

(1) A Hierarchical ascending cluster analysis (HAC) with Ward criterion was applied to the Euclidean distance matrix of the 27 normalized mean monthly NCEP/NCAR atmospheric variables (Ward, 1963). HAC has been applied in several climate studies, such as Vrac et al. (2007b) who categorized the regional climate conditions in the state of Illinois, USA, in terms of circulation and precipitation atmospheric patterns. By applying HAC in our study, the atmospheric variables which have the most similar "behaviours" have been grouped together within five homogeneous clusters related to precipitation, temperature, pressure, shortwave radiation and heat flux processes (Fig. 3a). The relevance of selecting five clusters was assessed using the silhouette information (SI) calculated for each variable, ranging from 0 to 1 for badly to perfectly clustered variables (Rousseeuw, 1987). In this study, the 27 variables were correctly placed within the five clusters (SI > 0.5). Furthermore, the five clusters represented physically meaningful information on well identified atmospheric processes.
(2) A principal component analysis (PCA) was applied to each of the five groups of variables to derive a physically meaningful and synthetic description of the given process. The first PC of each group, containing more than 80% of the total variance, was retained as predictor into the downscaling (Fig. 3b). The pairwise Pearson correlation between the first PC of each group was ensured not to exceed 0.7.

Statistical downscaling framework

Prior to the downscaling process, flow data were first standardized per station. For a given station, the annual mean flow was subtracted from the time series of daily flows and the result divided by the standard deviation of the daily flow time series. This was done to make the dimension of flow values comparable between stations. The standardized data were then transformed using

Table 3
Description of the NCEP/NCAR reanalysis predictors used into the downscaling framework for river flow simulation, with their acronyms and correspondence with global circulation models outputs.

NCEP names	NCEP short names	Pressure levels (hPa)	Units	Corresponding monthly GCM output	Corresponding daily GCM output
Mean daily air temperature	air	500, 850,1000	K	ta	ta
Mean daily convective precipitation rate at surface	cprat		kg m^{-2} s^{-1}	prc	
Mean daily clear sky downward longwave flux at surface	csdlf		W m^{-2}	rldscs	
Mean daily clear sky downward solar flux at surface	csdsf		W m^{-2}	rsdscs	
Mean daily clear sky upward solar flux at surface	csusf		W m^{-2}	rsuscs	
Mean daily downward longwave radiation flux at surface	dlwrf		W m^{-2}	rlds	rlds
Mean daily downward solar radiation flux at surface	dswrf		W m^{-2}	rsds	rsds
Mean daily geopotential height	hgt	500, 850, 1000	m	zg	zg
Mean daily upward longwave radiation flux at surface	ulwrf		W m^{-2}	rlus	rlus
Mean daily precipitation rate at surface	prate		kg m^{-2} s^{-1}	pr	pr
Mean daily surface pressure	pres		Pa	ps	ps
Mean daily relative humidity	rhum	500, 850, 1000	%	hur	
Mean daily upward solar radiation flux at surface	uswrf		W m^{-2}	rsus	rsus
Mean daily specific humidity	shum	500, 850, 1000	kg kg^{-1}	hus	hus
Mean daily SST/land skin Temperature	skt		K	ts	
Mean daily sea level pressure	slp		Pa	psl	psl
Mean daily total cloud cover	tcdc		%	clt	
Mean daily latent heat net flux at surface	lhtfl		W m^{-2}	hfls	hfls
Mean daily sensible heat net flux at surface	shtfl		W m^{-2}	hfss	hfls

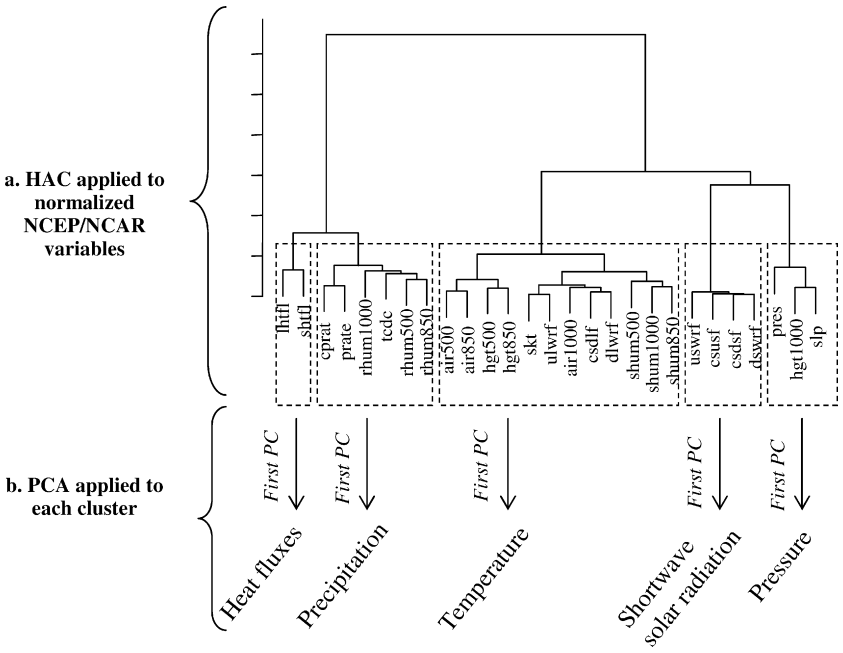

Fig. 3. Atmospheric predictors, namely heat flux, precipitation, temperature, shortwave solar radiation and pressure fields were derived from the 27 normalized NCEP/NCAR atmospheric variables. The atmospheric variables were first clustered (a) using hierarchical ascending analysis with Ward criterion (HAC), then process-based predictors were synthesized into the first component of a principal component analysis (PCA) applied to each cluster (b). The 27 variables are explained in Table 3.

box–cox power transformations to make the shape of the distribution as Gaussian as possible, so that the GLM and GAM assumption of normality was valid (Box and Cox, 1964). The whole analysis was made with the R statistical software and supporting routines that have been compiled into the DS package for R, available on request.

Point (P) and regional (R) downscaling

Point downscaling refers to the calibration of a statistical model to each of the 51 gauging stations. Regional downscaling, in this study, refers to the calibration of a statistical model to a group of gauging stations representative of a hydrological regime. These regimes were previously identified via HAC method with Ward criterion to group the 51 gauging stations into five homogeneous and well identified hydrological regimes ranging from nival to pluvial (Fig. 2). The five selected clusters were assumed to be the optimal number of clusters for the present analysis in comparison to a larger or smaller number of clusters. Thus all the stations from the same hydrological regime have the same calibrated model. HAC was applied to the Euclidean distance matrix of stations based on their standardized monthly flow percentiles (10%, 50% and 90%). Note that HAC was performed based on monthly flow percentiles only, and not other basin characteristics.

Daily (D) vs. fortnightly (F) direct downscaling vs. daily integrated downscaling (I)

The comparative downscaling framework includes three different time scale strategies (Fig. 1c). In this study, SDM aims at relating directly the daily mean (D) and fortnightly mean (F) atmospheric predictors, respectively to the daily mean flow and fortnightly flow statistics which were the fortnightly percentiles 10%, 50%, and 90%. Such indices have been applied in downscaling context to improve percentiles estimates, especially extremes (Dibike and Coulibaly, 2006). The fortnightly scale was preferred to monthly scale to increase the number of sampling units and improve the statistical inference.

The daily 'integrated' SDM (I) was based on two separate downscaling steps from the initial daily time series of flow. Firstly, the downscaling of the daily seasonal cycle was done; secondly, the downscaling of the corresponding daily anomalies. Finally, the downscaled daily seasonal cycle and anomalies are summed afterwards to complete the daily integrated approach. As such, downscaling the seasonal cycle aims at modelling the flow seasonality while downscaling the anomalies aims at modelling the variation around the daily seasonal cycle. A review of the literature suggests that such an approach has not been tried previously.

Statistical models

For each of the six SDM spatial/temporal combinations examining point and regional downscaling at each of the daily, fortnightly and 'integrated' time scales, GLM, GAM, ABT and ANN statistical methods were also compared for each of the six combinations (Fig. 1b).

Generalized linear and generalized additive models. Generalized Linear Models (GLM) are a flexible generalization of ordinary least squares regression, unifying various other statistical models, including linear, logistic and Poisson regression under one framework (McCullagh, 1984). In GLM, each outcome of the response variable Y (i.e., flow) is assumed to be generated from a particular distribution function in the exponential family that includes the normal, binomial and Poisson distributions. Flow data were assumed to be normally distributed after box-cox transformation. The mean of the distribution, μ, depends on the predictor variables X, namely the NCEP/NCAR predictors. The model was defined as:

$$g(E(Y|X)) = \beta X + \alpha \quad (1)$$

where $E(Y|X)$ is the expected value of Y conditionally on X; β and α corresponds respectively to a vector of unknown parameters to be estimated and the intercept; g is the function relating the predictors to the flow variable. The g function is called the "link" function and can take many shapes (determined by the user) in order to make applicable the right parts of Eq. (1). Indeed, according to the distribution family of Y, the link function g has to be changed. In the present study, the flow variability to downscale are assumed to be Gaussian distributed and then $E(Y|X)$ is directly related the right

parts of Eq. (1) (see Hastie and Tibshirani, 1990 for technical and theoretical details). Hence, g is taken as the identity function.

Generalized additive models (GAM) have been developed for extending properties of GLM to non-linear relationships between X and Y through additive properties (Hastie and Tibshirani, 1990). GAM fits the conditional expectation of Y given X, as the sum of m spline functions f_i of some or all of the covariates (Wood, 2008), where m is the dimension of X:

$$g(E(Y|X)) = \sum_{i=1}^{m} f_i(x_i) + \theta_0 \quad (2)$$

As for GLM, GAM specifies a distribution for the response variable. The functions f_i can be parametric or non-parametric, thus providing the potential for non-linear fits to the data which GLM does not allow. In this study, the spline functions, f_i, are defined as natural cubic splines, namely splines constructed of piecewise third-order polynomials with continuity conditions expressed until second derivatives (Hastie and Tibshirani, 1990). θ_0 is a constant to be estimated and g was defined as the identity function.

Feedforward artificial neural network. A multi-layer perceptron feedforward artificial neural network (ANN) was used in this study. This type of neural network is extremely flexible and has been applied to a wide variety of hydrological and climate situations (Reed and Marks, 1998). In this study the artificial neural network was trained using a back-propagation algorithm (Rumelhart et al., 1986). The architecture of the neural network used was three layers of neurons: the input layer, the hidden layer and the output layer. Every neuron of a layer was connected with every neuron of the previous layer by weight links that were modified during successive iterations. The value of the output from each neuron was calculated using the tanh sigmoid transfer function [$f(x) = 1/(1 + e^{-x})$]. The back-propagation algorithm adjusted the connection weights according to the back propagated error computed between the observed and the estimated results. This is a supervised training procedure that attempts to minimize the error between the desired and the predicted output (Lek and Guégan, 2000). The output Y from the neural network was given by:

$$Y = \sum_j \tan h\left(\sum_i x_i w_{i,j}^1 + b_j^1\right) w_j^2 + b^2 \quad (3)$$

where x_i represents the ith input predictors, $w_{i,j}^1$ and w_i^2 are the hidden input and output layer weights, and $b_{i,j}^1$ and b^2 the hidden input and output layer biases. Here, $j = 4$ internal nodes were chosen for the single-hidden layer by comparing the downscaling performances with a different number of nodes whose range was defined using the empirical formula (Huang and Foo, 2002):

$$\sqrt{2i} + o < j < 2i + 1 \quad (4)$$

Where i is the number of input nodes corresponding to the number of atmospheric predictors (i.e. in our case the five process-based predictors), o is the number of output nodes (i.e. in this study $o = 1$).

Aggregated boosted regression trees (ABT). There was no evidence in the readily-accessible literature that boosted trees have been used in downscaling studies. Friedman et al. (2000) and Hastie et al. (2001) introduced the technique for use in applied statistics, especially in ecological applications. Boosted trees are based on a compilation of classification and regression tree (CART) models. CART models explain variation of a single response variable by repeatedly splitting the data into more homogeneous groups, using combinations of explanatory variables that may be categorical and/or numeric. Each group is characterized by a typical value of the response variable, the number of observations in the group and the values of the explanatory variables that define it (De'ath and Fabricius, 2000).

The aim of boosted trees is to improve the performance of a single CART model by fitting m models, in our case 1000 models, where each successive CART is built for the prediction residuals of the preceding tree (Elith et al., 2008). Considering a loss function that represents the loss in predictive performance (e.g., deviance explained) between two models, boosting is a numerical optimization technique that minimizes the value of the loss function by adding, at each new step, a new CART that best reduces the loss function (Elith et al., 2008). To limit the over-fitting of the boosted trees caused by the construction of too many CART models, each new CART is grown on a randomized subset of the dataset. Then, the optimal number of trees is automatically selected, after the 1000 generated CART in our study, so that that the loss in predictive performance calculated on the remaining subset of the dataset was minimized (De'ath, 2007).

Aggregated boosted trees (ABT) are themselves an extension of boosted trees. Aggregated boosted trees comprise a collection of boosted trees generated on a cross-validation subset, which reduce the prediction error relative to a single boosted tree (De'ath, 2007).

Validation and evaluation of model performances

The same validation procedure was applied to all downscaling schemes. Observations were chosen from the whole sample to form the training dataset (the first 70% of each time series), and the remaining observations (i.e. corresponding to the last 30% of each time series) were retained as the validation dataset (Fig. 1d). Hence, validation and training datasets are temporally independent. For the comparison between the different spatial and time scales downscaling models, performance was evaluated using the coefficient of determination, R^2, calculated by station for each fortnightly statistics (percentiles 10%, 50% and 90% of flow) between observations (O) and simulations (S) from year i to n, through:

$$R^2 = \left\{ \frac{\sum_{i=1}^{n}(O_i - \overline{O})(S_i - \overline{S})}{\left[\sum_{i=1}^{n}(O_i - \overline{O})^2\right]^{0.5}\left[\sum_{i=1}^{n}(S_i - \overline{S})^2\right]^{0.5}} \right\} \quad (5)$$

R^2 values range from 0 (poor model) to 1 (perfect model). Statistical downscaling models with R^2 values above 0.5 will be interpreted here as good models, showing that 50% of the flow variability is explained by the atmospheric predictors (Fig. 1d).

Sensitivity of downscaled flows to atmospheric predictors

Based on the regional fortnightly downscaling approach, a sensitivity analysis was performed to quantify the contribution from each of the five process-based predictors to the explained variance of the river flow, according to the different hydrological regions and the four statistical methods, namely GLM, GAM, ANN and ABT. Since the core from the four statistical methods is based upon different algorithm, the sensitivity approach developed here to quantify the influence of predictors to the flow variability was specific to each statistical method. However, to make comparable the results between the four statistical methods, the percentage contribution of each predictor to the flow variance explained (i.e. R^2) is scaled so that the sum adds to 100, with higher numbers indicating stronger contribution to the response (Elith et al., 2008).

Sensitivity measure

For GAM and GLM, the sensitivity of flow variability to the atmospheric predictors was estimated via the Fisher–Snedecor

statistic, F, calculated for each of the predictors. Typically in GLM and GAM framework, the F statistic is the ratio of the explained variability by a given predictor (as calculated by the R^2 coefficient of determination) and the unexplained variability (as calculated by $1 - R^2$), divided by the corresponding degree of freedom (Lomax, 2007). Thus, the larger the F statistic, the more important is the predictor to flow variance explained.

For ANN, the influence predictor to the flow variability was evaluated via the method of partial derivates (Dimopoulos et al., 1995; Gevrey et al., 2003). With the method of partial derivates, the sum of square derivatives value was obtained per input variable and allowed a classification of the input variables according to their increasing contribution to the output variable (i.e. river flows) in the model. The input variable with the highest sum of square derivatives value was the variable most influencing the output variable.

For ABT, the flow sensitivity to each atmospheric predictor was assessed using the method described by Friedman (2001). The contribution of predictors is based on the number of times a predictor is selected for splitting during the boosting process, weighted by the squared improvement (i.e. the loss in predictive performance) to the model as a result of each of those splits, and averaged over all models.

Multivariate analysis of variance

Each downscaling model was performed 500 times using flow datasets of size 500 ($m = 500$), randomly drawn from the training dataset and representing approximately 25% of it. A Multivariate Analysis of Variance (Manova) was applied to test if the relative contribution of the five atmospheric predictors ($a = 5$) was significantly different between each statistical model ($s = 4$) and between each hydrological regime ($h = 5$). Manova is a direct extension of anova where the two tested variables of interest are not tested on a single continuous variable but on the distance matrix. Here, the Euclidean distance matrix was calculated from the $i \times a$ matrix of predictors contribution, where $i = m \times s \times h$.

Future projections

Based on the regional fortnightly downscaling approach, future projections of median flow conditions were performed to illustrate the ability of using the downscaling framework for future climate change impact studies. The future projections were based on the GCM cnrm-cm3 from Meteo-France according to two scenarios from the IPCC (Pachauri and Reisinger, 2007), namely scenarios A2 and B1. Three time periods, namely 2025–2050, 2050–2075 and 2075–2100 were investigated and the relative changes of flow (RC) were calculated seasonally for each station to highlight the contrasted changes between nival and pluvial regimes according to the two scenarios. RC was calculated as difference between future projected and observed (1970–2000) flow condition, divided by the observed condition. For example, a relative change of +0.20 indicates a future flow increase of 20%. The future flow projections were made in three steps:

The GCM atmospheric variables for the two future scenarios were standardized according to their control period, i.e. under the scenario '20c3m' which represents a simulation of the GCM over 1970–2000 based on historical trends. This was done to remove the potential bias in the mean and the standard deviation of GCM atmospheric variables over the period 1970–2000.

As many hydrological change impact studies (e.g., Hay et al., 2000), the delta method was applied to each of the 21 atmospheric variables by adding the change in climate to an observational database to represent the future climate. More specifically for a given station and a given month, the delta method was calculated as the mean difference between the observations, i.e. the averaged NCEP/NCAR conditions over 1970–2000, and the averaged GCM projections over a given future time period. Then the observations and the estimated mean difference were summed afterwards to recombine a future fortnightly times series of atmospheric variables.

The future fortnightly times series of the 21 atmospheric variables were then projected onto the first principal component axis from their respective group of atmospheric variables (see Section "Deriving process-based NCEP/NCAR predictors") to derive the four atmospheric predictors for the downscaling.

Results

The Hierarchical ascending cluster analysis applied to our 51 stations produced five hydrological regimes, ranging from nival to pluvial systems (Fig. 2). The nival regime characterizes stations mostly located in the headwaters of the Pyrenees (six stations) with the annual peak of flows generally occurring during the spring snowmelt. Conversely, the pluvial regime characterizes lowland stations (10 stations), influenced by heavy winter rainfall in the Massif Central leading to maximum annual flows in winter. Transitional nival to pluvial regimes are observed for intermediate stations collecting water both from Pyrenees and Central Massif (Fig. 2). The seasonal Pearson correlations between the observed flows and the corresponding process-based predictors, namely precipitation, temperature, solar radiations, heat fluxes and pressure PC (Fig. 3), show some seasonal correlations according to nival or pluvial regimes (Fig. 4). Temperature and shortwave solar radiations correlated with observed flows show the largest seasonal variability in the correlations (Fig. 4a and b). While the correlation between flow and temperature is globally negative in summer and autumn as well as weak in winter for both nival and pluvial regimes, the temperature in spring correlates flow negatively in pluvial systems and positively in nival ones (Fig. 4a). The seasonal correlation of flow with the shortwave solar radiations exhibits the same trends than those observed with the temperature, excepted in summer where the correlation between flow and the shortwave radiations remains positive for both pluvial and nival regimes (Fig. 4b). The correlation between precipitation and flows is globally positive throughout the year, approximately $R = 0.4$ (Fig. 4c). Heat fluxes and pressure predictors do not show strong seasonal correlations with flows, although flow correlation to the pressure PC averaged −0.2, nor major differences between nival and pluvial regimes (Fig. 4d and e).

The mean percentage contribution and standard deviation from the five process-based predictors to the flow variance explained was estimated for each statistical model (i.e. GLM, GAM, ABT, ANN) and per hydrological regime using the daily regional downscaling from 500 samples (Fig. 5). The Manova results show that the contribution of the atmospheric predictors was significantly different between the four statistical methods (Manova, $p < 0.001$) and between the five hydrological regimes (Manova, $p < 0.001$). Nival regimes are mainly driven by solar radiation fluxes whereas temperature is the key-process involved in pluvial regimes (Fig. 5a). Aggregated boosted trees seem to be more stable than other methods since the percentage of contribution calculated for each predictor show less variability then the one estimated from the GLM, GAM and ANN, as shown by the smaller amplitude in the boxplot (Fig. 5b). GLM, GAM and ANN emphasise the importance of temperature and solar radiation principal components to explain the flow variance. However, temperature and solar radiation remain the two most important factors for both statistical models (Fig. 5b).

Model performances (i.e. R^2 calculated between fortnightly observed and simulated flow statistics) were compared according to

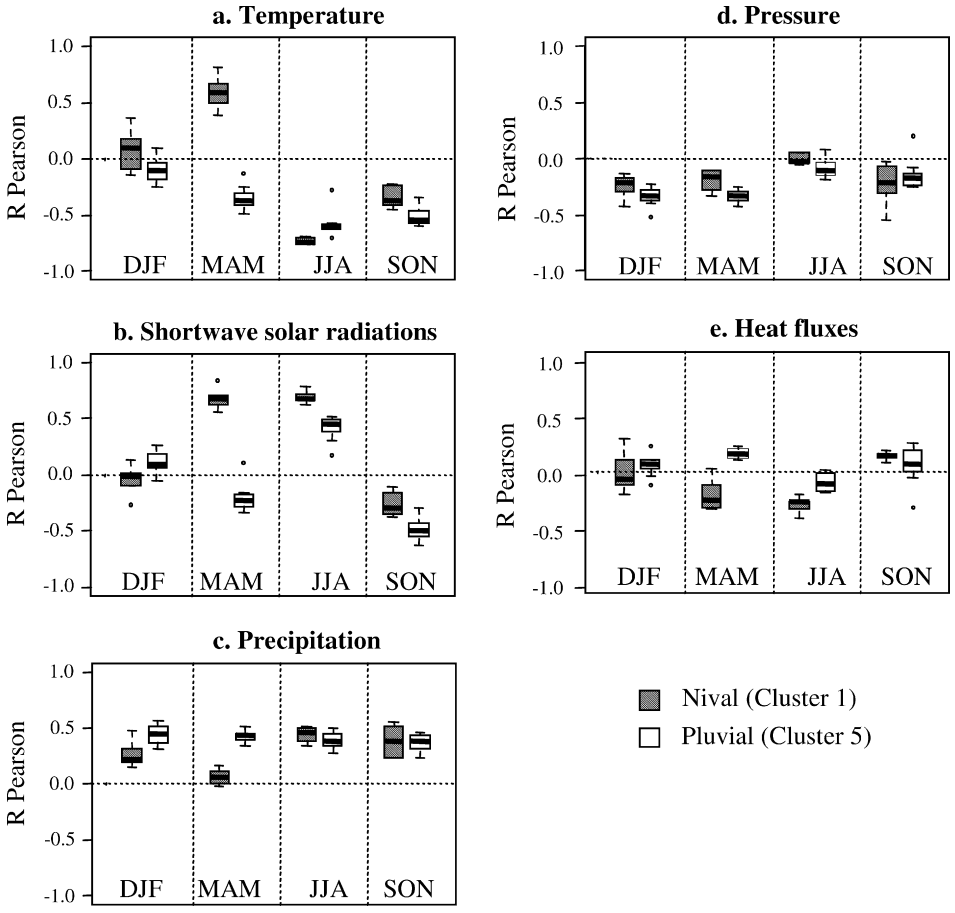

Fig. 4. Seasonal Pearson *R* correlation coefficients between flow and the five derived atmospheric predictors, as described in Fig. 3, according to nival (dark grey) and and pluvial (white) systems: (a) temperature, (b) shortwave solar radiation, (c) precipitation, (d) pressure and (e) heat fluxes.

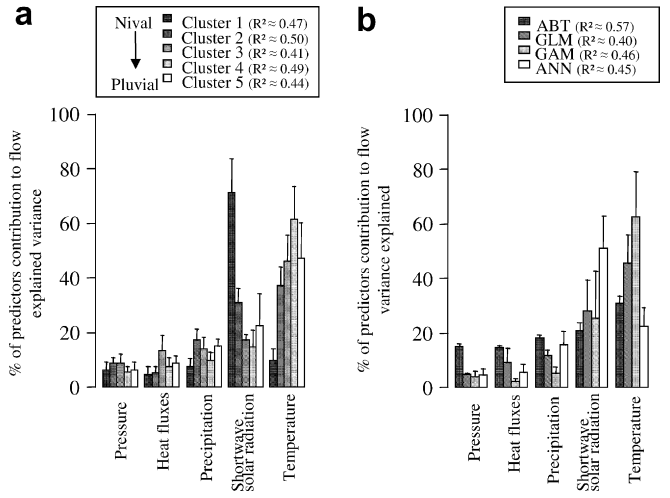

Fig. 5. Results of the sensitivity analysis showing the percentage contribution of the five atmospheric predictors to the explained flow variability, according to hydrological regimes (a) from nival (black) to pluvial (white); statistical downscaling models (b) ABT = aggregated boosted trees, GAM = generalized additive model, GLM = generalized linear model, ANN = artificial neural network.

each spatial/time scale combination, as well as according to the four statistical models and the five hydrological regimes. The results are presented in Fig. 6. Mean R^2 performances for aggregated boosted trees (ABT) are significantly better than those of the GLM (paired *t*-test, $p < 0.001$), GAM (paired *t*-test, $p < 0.001$) and ANN (paired *t*-test, $p < 0.001$), while GLM shows significantly lower performances (Fig. 6a; $R^2_{ABT} = 0.49$, $R^2_{GAM} = 0.44$, $R^2_{ANN} = 0.44$, $R^2_{GLM} = 0.40$. When averaging results from all methods, a slight decrease in high flow percentiles estimates is observed ($R^2_{p10} = 0.48$, $R^2_{p50} = 0.47$, $R^2_{p90} = 0.41$). Overall, fortnightly downscaling (F) slightly outperforms daily downscaling (D) and daily downscaling with integrated seasonal cycle and anomalies (I) ($R^2_F = 0.47$, $R^2_D = 0.43$, $R^2_I = 0.43$). Additional results from the daily integrated downscaling (not presented here) show its good performance in downscaling the seasonal cycle, but its lack of efficiency to simulate the daily anomalies. Point downscaling performs significantly better than the regional one as $R^2_{Point} = 0.51$ and $R^2_{Regional} = 0.46$ (paired *t*-test, $p < 0.001$) and it is significantly better for modelling high fortnightly flow percentiles (paired *t*-test, $p < 0.001$). The mean performance of downscaling models is lower in nival ($R^2_{cluster\ 1} = 0.41$) than in pluvial ($R^2_{cluster\ 5} = 0.45$) regimes, especially for high flow percentiles estimates (Fig. 6c; unpaired *t*-test, $p < 001$). Globally for the three percentiles, fortnightly flows is better simulated by the downscaling models in summer ($R^2_{JJA} = 0.28$) than in winter ($R^2_{DJF} = 0.11$), spring ($R^2_{MAM} = 0.16$) and autumn ($R^2_{SON} = 0.19$) (Fig. 6d).

Future projections in median flow conditions were performed based on the regional bimonthly downscaling approach and the ABT statistical method, according to two scenarios and analysed for three periods, namely 2025–2050, 2050–2075 and 2075–2100 (Fig. 7). Globally, the median flow conditions decrease in both nival (−17%) and pluvial (−15%) systems (Fig. 7a and b). In nival systems (Fig. 7a), this decrease is more particularly severe in spring

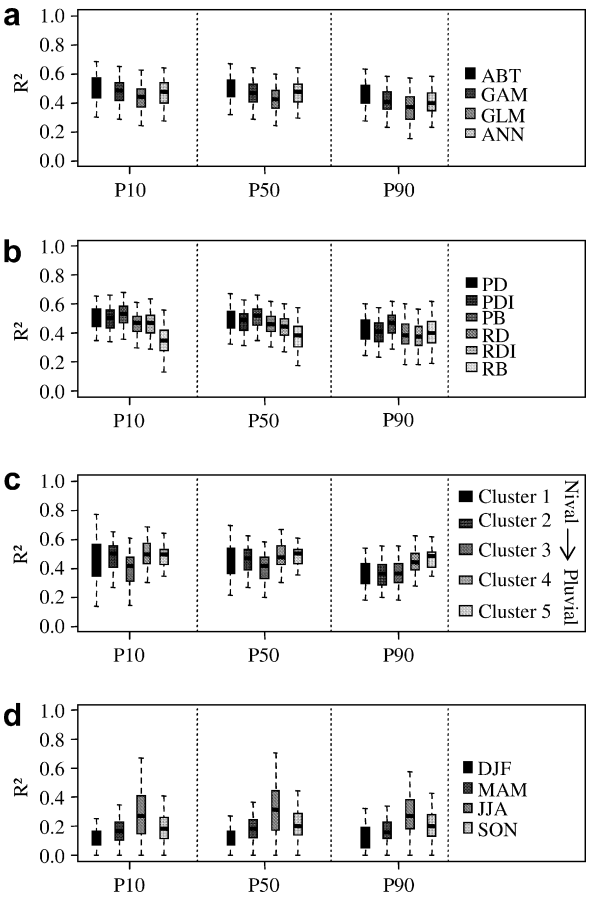

Fig. 6. Boxplot representing the variability in the performance of statistical downscaling models, as the variance explained (R^2) in modelling three fortnightly percentiles of river flow, namely percentiles 10% (P10), 10% (P50) and 90% (P90). Comparison is made between: (a) statistical downscaling models (ABT = aggregated boosted trees; GAM = generalized additive model; GLM = generalized linear model; ANN = artificial neural network); (b) downscaling approaches (PD = point daily downscaling; PI = point daily downscaling with integrated season and anomalies; PF = point fortnightly downscaling; RD = regional daily downscaling; RI = regional daily downscaling with integrated season and anomalies; RF = regional fortnightly downscaling); (c) hydrological regimes ranging from nival (cluster 1; dark grey) to pluvial (cluster 5; white); (b) seasons, namely winter (DJF), spring (MAM), summer (JJA) and autumn (SON).

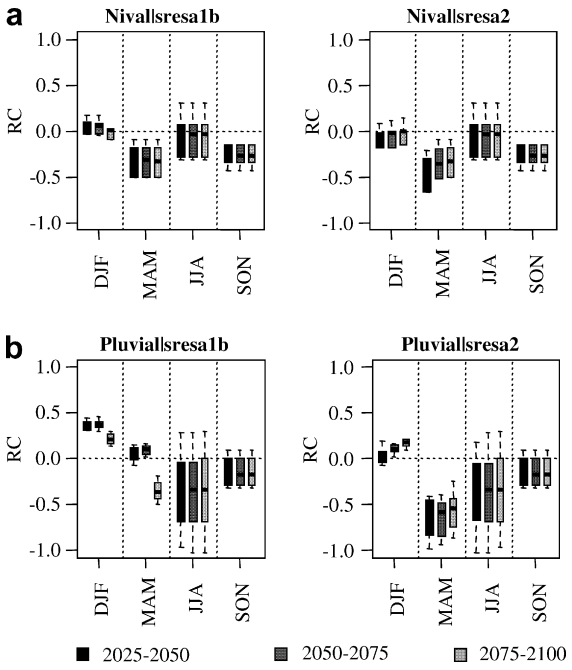

Fig. 7. Future relative changes (RC) in seasonal flow conditions projected for nival (a) and pluvial (b) regimes. Relative changes are highlighted for three periods, namely 2025–2050 (black), 2050–2075 (grey) and 2075–2100 (light grey) according to scenarios A2 and A1B.

($RC_{MAM} = -40\%$) and autumn ($RC_{SON} = -24\%$) than in winter ($RC_{DJF} = -7\%$) and summer ($RC_{JJA} = -7\%$). The future relative change of flows in nival systems is not significantly different between the A2 and A1B scenarios (paired t-test, $p = 0.32$) nor between the different periods (one-way Anova, $p = 0.45$). In pluvial systems (Fig. 7b), flows could globally increase in winter ($RC_{DJF} = +20\%$) while decreasing during the other seasons ($RC_{MAM} = -30\%$, $RC_{JJA} = -32\%$ and $RC_{SON} = -26\%$). The relative changes in pluvial systems are relatively the same according to the A2 and A1B scenarios, excepted in spring where flows decrease dramatically under the A2 scenario (Fig. 7b; $RC_{MAM} = -50\%$). Globally for both scenarios, the relative changes of flows in pluvial systems are significantly different between the three periods in winter only (Fig. 7b; one-way Anova; $p < 001$).

Discussion

The discussion will address the three main questions mentioned in the Introduction. Firstly, the technical aspects related to the different downscaling strategies will be discussed to highlight their main strengths and limits as well as some possibilities of improvements. Secondly, the reliability of the downscaling framework will be discussed in regards to the physical meaning linking atmospheric factors to streamflow variability according to nival and pluvial hydrological systems. Thirdly, future flow projections in nival and pluvial systems will be analysed to illustrate the applicability of the downscaling framework for future climate change impact studies.

Comparison between the different statistical downscaling strategies

In this study, a direct statistical downscaling approach from GCM to streamflow variability was experimented, which is less commonly applied than the approach involving an intermediate hydrological model between GCM and streamflow to reproduce the hydrological cycle (Fowler et al., 2007). While a direct downscaling approach may allow the assessment of the relationship between flow and atmospheric process over large spatial scales more easily than if using an intermediate hydrological model, some limits should be considered. Particularly, the direct downscaling approach was developed from a deterministic point of view by assuming that the variability of streamflow was influenced by climate factors only. Thus the direct downscaling approach developed in this study do not explicitly take into account for some physical factors, such as the land use and soil cover, which interact with climate and influence flow-pathways (e.g., interception, infiltration and groundwater processes) and may vary under future climate. In this context, using a hydrological model that classically integrates those physical factors within a delimited structure of the river catchment (e.g., HBV; Lindstrom et al., 1997) may provide a more realistic projection of the potential future hydrological conditions than the use of a direct downscaling approach. However, by comparing different statistical downscaling approaches according to different spatial/time scale strategies and statistical models, our study has revealed three key results encouraging further developments for the use of direct statistical downscaling approaches to assess the potential impact of climate change on hydrological resources.

Firstly, the downscaling performances using the regional approach did not deteriorate too much the quality of the projected fortnightly statistics in comparison to the point downscaling. This makes the regional approach very attractive from a technical point of view as well as for the understanding of large-scale hydro-climatic processes. Technically, the regional approach is 10 times faster to compute than the local one, approximately 30 min on a regular computer to calibrate the four statistical methods. Furthermore, the regional approach has shown to summarize satisfactorily the key relationship between climate and streamflow variability according to the different hydrological systems ranging from nival to pluvial. These two specificities make the regional approach of particular interest to extend feasibly the downscaling framework of streamflow across Europe. Finally, a few additional features could be added to the regional downscaling approach to improve the regional flow projections from GCM outputs, such as integrating the land cover, geology and soil covers to better identify hydrological region. The spatial autocorrelation between hydrological sites could be also integrated into a statistical downscaling framework of streamflow, which has never been done to our knowledge, for example to help projecting the flow variability from atmospheric process to ungauged hydrological stations.

Secondly, the fortnightly flow percentiles downscaling recorded better performances than daily and daily integrated downscaling, especially for high flow percentiles. These results are in agreement with studies focused on the downscaling of extreme climate events which highlighted good performances when downscaling seasonal extreme indices derived from daily climate data (Moberg and Jones, 2005; Hanson et al., 2007). The daily direct and daily integrated downscaling simulations were shown to reproduce accurately the daily flow seasonal cycle across the study area but failed to simulate the magnitude of high flow events. The difficulty for those two daily approaches to simulate high flow events may come from the statistical inability of models to relate high flow events to climate processes. Since high flow events may result from local climate processes and controlling processes such as localised convective precipitation or orographically, enhanced precipitation and thus the simulation of extreme floods from large-scale atmospheric conditions may not be satisfactorily simulated. The proposed downscaling of daily anomalies suffered the incapacity of the models to take into account for the seasonal variation in the relationship between the daily mean atmospheric processes and the daily anomalies. Thus, the downscaling of daily anomalies could be improved by possibly adding a seasonal signal (e.g., sin and cosin values related to the different months) to relate the daily mean atmospheric processes to the daily anomalies at a given season; or, even more simply, by conditioning the downscaling model per season. Moreover, the downscaling of daily anomalies could also take advantage of the extreme value theory (Coles, 2001; Katz et al., 2002; Vrac and Naveau, 2007) to improve high percentiles simulations. Recent studies have also characterized drought and floods at the daily time scale in relation to circulation patterns using fuzzy coding (e.g., Bardossy et al., 1995; Samaniego and Bardossy, 2007).

Secondly, the non-linear statistical models such as aggregated boosted tree, generalized additive models and artificial neural networks performed better than the generalized linear models to project the hydrological variability from atmospheric processes. Some similar results have been highlighted by Cannon and Whitfield (2002) and Ghosh and Mujumdar (2008) who respectively applied an ensemble of neural networks and support vectors machines to forecast streamflow from atmospheric processes. Although all three non-linear statistical models performed comparably in our study, the best performance was obtained for the aggregated boosted trees models. To our knowledge, this study is the first application of the aggregated boosted tree method for climate downscaling studies. However, earlier studies from Elith et al. (2008) and De'ath (2007) in ecology confirmed the relatively higher predictive power of boosted trees than that of other statistical methods. Anyway, since none statistical method may definitely assumed to be the best one, especially for climate change impact studies, it would worth to take into the uncertainty in downscaling projections from different statistical methods.

Relationship between atmospheric factors and streamflow variability

The hydrological response in catchments results from the complex interactions between hydro-climatic conditions, for example rainfall intensity and duration and the condition of soil moisture preceding a rainfall event, and the physical characteristics of the catchment, namely the land cover, the morphology of the river network and the soil characteristics. The hydrological cycle may be viewed as a balance between the evaporation and precipitation processes which drive the dynamics of water and the active flow-pathways regulating the soil moisture, the infiltration, groundwater recharge and surface runoff (Sun and Pinker, 2004; Li et al., 2007).

Atmospheric processes are generally related to river flows through atmospheric weather regimes (Kingston et al., 2006). Atmospheric weather regimes characterize the large spatial scale structure of a given atmospheric variable, often geopotential height, sea level pressure or specific humidity at different atmospheric levels, which are then used to relate flow dynamics. This was done by Kingston et al. (2006) in Britain; Stewart et al. (2005) and Molnár and Ramírez (2001) in north-western New Mexico; Anctil and Coulibaly (2004) and Déry and Wood (2004) in Canada; Krepper et al. (2003) in Uruguay; Lawler et al. (2003) in south-west Iceland; Struglia et al. (2004) across the Mediterranean region; and Ye et al. (2004) in Siberia.

In this study, a simplified representation of the relationship between atmospheric fields and flow generation was developed throughout five synthetic regional atmospheric factors derived from clustering and principal component analysis. Those five factors were related to precipitation, pressure, temperature, shortwave solar radiation and heat flux and they may show different or combined effect on the hydrological cycle. For example, evaporation mainly depends on the energy available in the system (e.g., heat fluxes, temperature, shortwave radiations) as well as the capacity of the air to store water (e.g., the pressure of water saturation in the air influence the air relative humidity). Similarly, precipitation results from a change in temperature and/or pressure, conditioned by a sufficient air relative humidity (Hufty, 2001). The sensitivity analysis of flow to those five atmospheric predictors revealed that pluvial and nival systems were mostly driven by temperature and shortwave solar radiation, i.e. by evaporation processes, more than by precipitation. Such results are in agreement with those of Phillips et al. (2003), who highlighted the main influence of regional temperature on flow in two pluvial rivers in southern Britain. Furthermore, the influence of temperature and shortwave radiation on streamflow variability showed some differences between nival and pluvial regimes.

In pluvial regimes, precipitation tends to fall as rain all year and the air temperature is negatively correlated to flow all year. That is, an increase in air temperature tends to actively increase the evaporation process and reduce the soil moisture, as shown by the negative correlation between the mean air temperature and flow in summer. In winter, the evaporation is reduced while the frequency and the intensity of precipitation increases, which leads to a saturation of the soil and higher groundwater levels. Thus, rainfall in winter is likely to contribute directly to a rising flow when the catchment is saturated, as shown by the positive correlation between the mean precipitation and flow in pluvial catchments.

Conversely in nival catchments, winter precipitation are generally stored as snow until spring, which do not contribute to soil

moisture saturation and do not consequently lead a rising flow, as confirmed by a very weak are correlation between mean precipitation and flow in winter (Fig. 4c). From spring, the rising shortwave solar radiations and temperature triggers snowmelt and typically generates a flow increase in nival systems, which may continue until summer. Shortwave solar radiations remain positively correlated to flow in spring and summer (Fig. 4b), possibly indicating a stronger control than temperature on the snowmelt process, as confirmed by some recent studies on snowmelt runoff modelling (Li and Williams, 2008).

Globally, high flows were less well simulated in nival systems than in pluvial ones. Although, the shortwave radiation and temperature were shown to be important processes for trigging the snowmelt from spring to summer, the prediction of high flows from snowmelt remains very difficult. This may be due to an inability for the downscaling models to capture the subtleties of snow-pack accumulation over the winter, ripening and melt.

Future hydrological projections in nival and pluvial systems

The suitability of the downscaling framework for future climate change impact studies was illustrated using a single statistical method, namely the aggregative boosted trees, and the regional approach to highlight how the nival and pluvial systems may respond to future climate change over the region. The interpretation of these future projections should be considered carefully since only one GCM model was used to characterize the future climate. Furthermore, the relevance of hydrological projections could be also criticized by the delta method used to derive the future atmospheric predictors for the regional downscaling. A major disadvantage of the delta approach is that representation of extremes from future climate scenarios effectively gets filtered out in the transfer process. The extremes resulting from this approach are simply the extremes from present climate observations that have either been enhanced or dampened according to the delta factors (Graham et al., 2007).

Globally, streamflow could decrease in both nival and pluvial systems over the region of study. In nival systems, the decrease of flow could be particularly important in spring while the precipitation and temperature increases could lead to the snow cover storage reduction and to an earlier melt (Caballero et al., 2007). In pluvial regimes, the rising precipitation in winter could be related to the dramatic increase of streamflow in winter. These results are in agreement with Caballero et al. (2007) who assessed the potential future changes of flows based on the mechanistic hydrological model, SAFRAN-ISBA-MODCOU (SIM), applied to the Adour-Garonne basin. However, recent applications of the SIM models over the same region highlighted a global diminution of precipitation all over the year leading to likely the same global diminution of flows all over the year (Boe et al., 2009).

Conclusion and wider perspective

To our knowledge, this study is one of the first one to compare extensively a number of statistical downscaling approach to project the hydrological variability directly from GCM atmospheric processes for a wide range of hydrological conditions. A first important result showed the ability of the downscaling modelling framework to highlight the contrasted dynamics of streamflow variability in nival and pluvial systems in response to key atmospheric processes. The results also emphasised the particular interest of using a regional approach to downscale directly the hydrological variability from GCM, for three reasons at least: (i) the capacity to capture the key relationship between the atmospheric and hydrological variability within each hydrological system; (ii) the possibility to extend feasibly the downscaling approach to higher spatial scales such as Europe; (iii) the possibility to improve the approach by taking into account for the spatial autocorrelation between sites or adding physical information to better help identifying hydrological regions or projecting hydrological changes at ungauged sites. This study was also the first application of the aggregated boosted trees method in statistical downscaling studies of hydro-climatology. That is, the aggregated boosted trees appeared to be the most efficient and stable method for modelling river flows in this case study, in comparison to others methods such as generalized linear models, generalized additive models and neural networks.

The main objective of this study was essentially to build and validate a downscaling framework of river flow directly from GCM outputs, to be used for future climate change impact studies. Thus, results from the projected future changes in the hydrology between nival and pluvial regimes were preliminary; however they were sufficiently encouraging to further development in the downscaling of river flow. For example, an ensemble method could be developed to downscale seasonal forecasts or future hydrological changes in different hydrological systems, by using several GCM, downscaling methods and different scenarios. Although this type of ensemble procedure has already been applied in several future hydrological studies based on an hydrological model to make the connection between downscaled climate conditions to river streamflow (Graham et al., 2007; Boe et al., 2009; Hagemann et al., 2009; Kay et al., 2009; Tapiador et al., 2009), to our knowledge it has never been applied to direct statistical downscaling framework of river flow from GCM. Further investigations are also under progress to build an integrated model chain linking the directly downscaled hydro-climatic conditions from GCM to some ecological models e.g., to project the potential impact of future hydro-climatic changes on the river ecosystem, from the nutrient loads to the structure of hydro-biological organisms.

Acknowledgements

This work was done as part of the EU FP6 Integrated Project "EURO-LIMPACS" (GOCE-CT-2003-505540) and GIS-REGYNA project. We thank J.-L. Le Rohellec (DIREN) for providing flow data; and National Oceanic and Atmospheric Administration (NOAA) for NCEP/NCAR reanalysis. We also thank the two anonymous referees for their insightful comments on an earlier draft of this manuscript.

References

Anctil, F., Coulibaly, P., 2004. Wavelet analysis of the interannual variability in southern Québec streamflow. Journal of Climate 17 (1), 163–173.
Arheimer, B., Wittgren, H.B., 1994. Modeling the effects of wetlands on regional nitrogen transport. Ambio 23 (6), 378–386.
Bardossy, A., Duckstein, L., Bogardi, I., 1995. Fuzzy rule-based classification of atmospheric circulation patterns. International Journal of Climatology 15 (10), 1087–1097.
Boe, J., Terray, L., Martin, E., Habets, F., 2009. Projected changes in components of the hydrological cycle in French river basins during the 21st century. Water Resources Research 45, W08426.
Box, G.E.P., Cox, D.R., 1964. An analysis of transformations. Journal of the Royal Statistical Society. Series B (Methodological) 23 (1), 211–252.
Caballero, Y., Voirin-Morel, S., Habets, F., Noilhan, J., LeMoigne, P., Lehenaff, A., Boone, A., 2007. Hydrological sensitivity of the Adour-Garonne river basin to climate change. Water Resources Research 43 (7), W07448.
Cannon, A.J., Whitfield, P.H., 2002. Downscaling recent streamflow conditions in British Columbia, Canada using ensemble neural network models. Journal of Hydrology 259 (1–4), 136–151.
Coles, S., 2001. An Introduction to Statistical Modeling of Extreme Values. Springer, London.
De'ath, G., 2007. Boosted trees for ecological modeling and prediction. Ecology 88 (1), 243–251.
De'ath, G., Fabricius, K.E., 2000. Classification and regression trees: a powerful yet simple technique for ecological data analysis. Ecology 81 (11), 3178–3192.
Déry, S.J., Wood, E.F., 2004. Teleconnection between the Arctic Oscillation and Hudson Bay river discharge. Geophysical Research Letters 31, 18.

Dibike, Y.B., Coulibaly, P., 2006. Temporal neural networks for downscaling climate variability and extremes. Neural Networks 19 (2), 135–144.
Dimopoulos, Y., Bourret, P., Lek, S., 1995. Use of some sensitivity criteria for choosing networks with good generalization ability. Neural Processing Letters 2 (6), 1–4.
Eckhardt, K., Fohrer, N., Frede, H.G., 2005. Automatic model calibration. Hydrological Processes 19 (3), 651–658.
Elith, J., Leathwick, J.R., Hastie, T., 2008. A working guide to boosted regression trees. Journal of Animal Ecology 77 (4), 802–813.
Fowler, H.J., Blenkinsop, S., Tebaldi, C., 2007. Linking climate change modelling to impacts studies: recent advances in downscaling techniques for hydrological modelling. International Journal of Climatology 27 (12), 1547–1578.
Friedman, J.H., 2001. Greedy function approximation: a gradient boosting machine. The Annals of Statistics 29 (5), 1189–1232.
Friedman, J., Hastie, T., Tibshirani, R., 2000. Additive logistic regression: a statistical view of boosting. The Annals of Statistics 28 (2), 337–407.
Gevrey, M., Dimopoulos, L., Lek, S., 2003. Review and comparison of methods to study the contribution of variables in artificial neural network models. Ecological Modelling 160 (3), 249–264.
Ghosh, S., Mujumdar, P.P., 2008. Statistical downscaling of GCM simulations to streamflow using relevance vector machine. Advances in Water Resources 31 (1), 132–146.
Graham, L.P., Hagemann, S., Jaun, S., Beniston, M., 2007. On interpreting hydrological change from regional climate models. Climatic Change 81, 97–122.
Habets, F., Boone, A., Champeaux, J.L., Etchevers, P., Franchisteguy, L., Leblois, E., Ledoux, E., Le Moigne, P., Martin, E., Morel, S., Noilhan, J., Segui, P.Q., Rousset-Regimbeau, F., Viennot, P., 2008. The SAFRAN-ISBA-MODCOU hydrometeorological model applied over France. Journal of Geophysical Research Atmospheres 113 (D6), D06113.
Hagemann, S., Göttel, H., Jacob, D., Lorenz, P., Roeckner, E., 2009. Improved regional scale processes reflected in projected hydrological changes over large European catchments. Climate Dynamics 32 (6), 767–781.
Hanson, C.E., Palutikof, J.P., Livermore, M.T.J., Barring, L., Bindi, M., Corte-Real, J., Durao, R., Giannakopoulos, C., Good, P., Holt, T., Kundzewicz, Z., Leckebusch, G.C., Moriondo, M., Radziejewski, M., Santos, J., Schlyter, P., Schwarb, M., Stjernquist, I., Ulbrich, U., 2007. Modelling the impact of climate extremes: an overview of the MICE project. Climatic Change 81, 163–177.
Harpham, C., Wilby, R.L., 2005. Multi-site downscaling of heavy daily precipitation occurrence and amounts. Journal of Hydrology 312 (1–4), 235–255.
Hastie, T.J., Tibshirani, R.J., 1990. Generalized Additive Models, Monographs on Statistics and Applied Probability, vol. 43. Chapman & Hall 9, 41.
Hastie, T.J., Tibshirani, R.J., Friedman, J.H., 2001. The Elements of Statistical Learning. Springer-Verlag, New York.
Hay, L.E., Wilby, R.J.L., Leavesley, G.H., 2000. A comparison of delta change and downscaled GCM scenarios for three mountainous basins in the United States. Journal of the American Water Resources Association 36 (2), 387–397.
Hewitson, B., 1994. Regional climates in the GISS general circulation model: surface air temperature. Journal of Climate 7 (2), 283–303.
Huang, W., Foo, S., 2002. Neural network modeling of salinity variation in Apalachicola River. Water Research 36 (1), 356–362.
Hufty, A., 2001. Introduction à la Climatologie. De Boeck University, Bruxelles. 541 pp.
Huth, R., Kliegrova, S., Metelka, L., 2008. Non-linearity in statistical downscaling: does it bring an improvement for daily temperature in Europe? International Journal of Climatology 28 (4), 465–477.
Kalnay, E., Kanamitsu, M., Kistler, R., Collins, W., Deaven, D., Gandin, L., Iredell, M., Saha, S., White, G., Woollen, J., Zhu, Y., Chelliah, M., Ebisuzaki, W., Higgins, W., Janowiak, J., Mo, K.C., Ropelewski, C., Wang, J., Leetmaa, A., Reynolds, R., Jenne, Roy., Joseph, Dennis., 1996. The NCEP/NCAR 40-year reanalysis project. Bulletin of the American Meteorological Society 77 (3), 437–471.
Katz, R.W., Parlange, M.B., Naveau, P., 2002. Statistics of extremes in hydrology. Advances in Water Resources 25 (8–12), 1287–1304.
Kay, A.L., Davies, H.N., Bell, V.A., Jones, R.G., 2009. Comparison of uncertainty sources for climate change impacts: flood frequency in England. Climatic Change 92 (1–2), 41–63.
Khan, M.S., Coulibaly, P., Dibike, Y., 2006. Uncertainty analysis of statistical downscaling methods. Journal of Hydrology 319 (1–4), 357–382.
Kingston, D.G., Lawler, D.M., McGregor, G.R., 2006. Linkages between atmospheric circulation, climate and streamflow in the northern North Atlantic: research prospects. Progress in Physical Geography 30 (2), 143–174.
Krepper, C.M., Garcia, N.O., Jones, P.D., 2003. Interannual variability in the Uruguay river basin. International Journal of Climatology 23 (1), 103–115.
Landman, W.A., Mason, S.J., Tyson, P.D., Tennant, W.J., 2001. Statistical downscaling of GCM simulations to streamflow. Journal of Hydrology 252 (1–4), 221–236.
Lawler, D.M., McGregor, G.R., Phillips, I.D., 2003. Influence of atmospheric circulation changes and regional climate variability on river flow and suspended sediment fluxes in southern Iceland. Hydrological Processes 17 (16), 3195–3223.
Lek, S., Guégan, J.F., 2000. Artificial Neuronal Networks: Application to Ecology and Evolution. Springer, Berlin.
Li, X.G., Williams, M.W., 2008. Snowmelt runoff modelling in an arid mountain watershed, Tarim Basin, China. Hydrological Processes 22 (19), 3931–3940.
Li, H., Robock, A., Wild, M., 2007. Evaluation of intergovernmental panel on climate change fourth assessment soil moisture simulations for the second half of the twentieth century. Journal of Geophysical Research 112, D06106.
Lindstrom, G., Johansson, B., Persson, M., Gardelin, M., Bergstrom, S., 1997. Development and test of the distributed HBV-96 hydrological model. Journal of Hydrology 201 (1–4), 272–288.
Lomax, R.G., 2007. An Introduction to Statistical Concepts. Lawrence Erlbaum.
McCullagh, P., 1984. Generalized linear-models. European Journal of Operational Research 16 (3), 285–292.
Moberg, A., Jones, P.D., 2005. Trends in indices for extremes in daily temperature and precipitation in central and western Europe, 1901–1999. International Journal of Climatology 25 (9), 1149–1171.
Molnár, P., Ramírez, J.A., 2001. Recent trends in precipitation and streamflow in the Rio Puerco Basin. Journal of Climate 14 (10), 2317–2328.
Pachauri, R.K., Reisinger, A., 2007. Climate Change 2007: Synthesis Report. Contribution of Working Groups I, II and III to the Fourth Assessment Report of the Intergovernmental Panel on Climate Change. Geneva, Switzerland.
Phillips, I.D., McGregor, G.R., Wilson, C.J., Bower, D., Hannah, D.M., 2003. Regional climate and atmospheric circulation controls on the discharge of two British rivers, 1974–1997. Theoretical and Applied Climatology 76 (3), 141–164.
Prudhomme, C., Reynard, N., Crooks, S., 2002. Downscaling of global climate models for flood frequency analysis: where are we now? Hydrological Processes 16 (6), 1137–1150.
Reed, R.D., Marks, R.J., 1998. Neural Smithing: Supervised Learning in Feedforward Artificial Neural Networks. MIT Press Cambridge, MA, USA.
Rousseeuw, P.J., 1987. Silhouettes – a graphical aid to the interpretation and validation of cluster-analysis. Journal of Computational and Applied Mathematics 20, 53–65.
Rumelhart, D.E., Hintont, G.E., Williams, R.J., 1986. Learning representations by back-propagating errors. Nature 323 (6088), 533–536.
Salameh, T., Drobinski, P., Vrac, M., Naveau, P., 2009. Statistical downscaling of near-surface wind over complex terrain in southern France. Meteorology and Atmospheric Physics 103 (1), 253–265.
Samaniego, L., Bardossy, A., 2007. Relating macroclimatic circulation patterns with characteristics of floods and droughts at the mesoscale. Journal of Hydrology 335 (1–2), 109–123.
Schnur, R., Lettenmaier, D.P., 1998. A case study of statistical downscaling in Australia using weather classification by recursive partitioning. Journal of Hydrology 213 (1–4), 362–379.
Stewart, I.T., Cayan, D.R., Dettinger, M.D., 2005. Changes toward earlier streamflow timing across western North America. Journal of Climate 18 (8), 1136–1155.
Struglia, M.V., Mariotti, A., Filograsso, A., 2004. River discharge into the mediterranean sea: climatology and aspects of the observed variability. Journal of Climate 17 (24), 4740–4751.
Sun, D., Pinker, R.T., 2004. Case study of soil moisture effect on land surface temperature retrieval. Geoscience and Remote Sensing Letters IEEE 1 (2), 127–130.
Tapiador, F.J., Sanchez, E., Romera, R., 2009. Exploiting an ensemble of regional climate models to provide robust estimates of projected changes in monthly temperature and precipitation probability distribution functions. Tellus Series A – Dynamic Meteorology and Oceanography 61 (1), 57–71.
Thompson, J.R., Sørenson, H.R., Gavin, H., Refsgaard, A., 2004. Application of the coupled MIKE SHE/MIKE 11 modelling system to a lowland wet grassland in southeast England. Journal of Hydrology 293 (1–4), 151–179.
Vrac, M., Naveau, P., 2007. Stochastic downscaling of precipitation: From dry events to heavy rainfalls. Water Resources Research 43 (7), W07402.
Vrac, M., Marbaix, P., Paillard, D., Naveau, P., 2007a. Non-linear statistical downscaling of present and LGM precipitation and temperatures over Europe. Climate of the Past 3, 669–682.
Vrac, M., Stein, M., Hayhoe, K., 2007b. Statistical downscaling of precipitation through nonhomogeneous stochastic weather typing. Climate Research 34 (3), 169–184.
Ward, J., 1963. Hierarchical grouping to optimize an objective function. Journal of the American Statistical Association 58, 236–244.
Whitehead, P.G., Wilby, R.L., Battarbee, R.W., Kernan, M., Wade, A.J., 2009. A review of the potential impacts of climate change on surface water quality. Hydrological Sciences Journal 54 (1), 101–123.
Wilby, R.L., Hay, L.E., Leavesley, G.H., 1999. A comparison of downscaled and raw GCM output: implications for climate change scenarios in the San Juan River basin, Colorado. Journal of Hydrology 225 (1–2), 67–91.
Wilby, R.L., Dawson, C.W., Barrow, E.M., 2002. Sdsm-a decision support tool for the assessment of regional climate change impacts. Environmental Modelling and Software 17 (2), 145–157.
Wood, S.N., 2008. Fast stable direct fitting and smoothness selection for generalized additive models. Journal of the Royal Statistical Society Series B – Statistical Methodology 70, 495–518.
Xu, C.Y., 1999. From GCM to river flow: a review of downscaling methods and hydrologic modelling approaches. Progress in Physical Geography 23 (2), 229–249.
Ye, H., Yang, D., Zhang, T., Zhang, X., Ladochy, S., Ellison, M., 2004. The impact of climatic conditions on seasonal river discharges in Siberia. Journal of Hydrometeorology 5 (2), 286–295.
Zorita, E., von Storch, H., 1999. The analog method as a simple statistical downscaling technique: comparison with more complicated methods. Journal of Climate 12 (8), 2474–2489.